Nearly Monodisperse Cu_2O and CuO Nanospheres: Preparation and Applications for Sensitive Gas Sensors

Jiatao Zhang, Junfeng Liu, Qing Peng, Xun Wang, and Yadong Li*

Department of Chemistry, Tsinghua University, Beijing 100084, People's Republic of China

Received October 12, 2005
Revised Manuscript Received January 13, 2006

Monodisperse nanospheres and spherical structures derived from them, such as core−shell or hollow nanospheres, have become a new study focus because their potential applications in optics, electrics, catalysis, sensors, and so forth.[1−4] Many researchers are working on the preparation of new monodisperse nanospheres and their functional transformation.[5−14] The traditional monodisperse micro- or nanospheres are amorphous silica and polymer colloids which were prepared by controlled hydrolyzation of tetraethyl orthosilicate and emulsion polymerization.[5−8] Using these colloidal templates, the Caruso group has prepared many kinds of porous hollow spheres and core−shell nanospheres through the "layer-by-layer" method, such as coating the spheres with noble-metal nanoparticles, metal oxide nanoparticles, polyelectrolytes, or biomolecules with specific electronic, optical, catalytic, and biological applications.[2,10] In recent years, much progress has been made on the preparation of monodisperse inorganic nanospheres.[11−13] For example, the Xia group has developed the glycol refluxing method to synthesize monodisperse metal micro or nanospheres, such as Bi, Pb, Se, metal alloys, and their functional core−shell structures.[11] Our group has developed the hydrothermal or solvothermal method to synthesize monodisperse micro- and nanospheres, such as chalcogenide, carbon, single-crystalline magnetic ferrite, and so forth.[12−14] By the template of carbon colloids, many hollow spheres, such as Ga_2O_3, GaN, WO_3, and so forth have been prepared with special optical or sensor properties.[14] From above, it is concluded that because the intrinsic properties of monodisperse nanospheres can be finely tuned by changing parameters such as diameter, chemical composition, bulk structure, and crystallinity, searching for novel methods and preparing more kinds of monodisperse nanospheres are still required for some special applications.[6]

Cuprous oxide (Cu_2O), a p-type semiconductor with unique optical and magnetic properties, has potential applications in solar energy conversion, electronics, magnetic storage, catalysis, and gas sensors. CuO is also a potential material with many applications in catalysis, gas sensing, and lithium−copper oxide electrochemical cells.[15−18] CuO was the first kind of humidity sensing material found by Braver et al. in 1931. It was reported that Cu_2O films had gas sensing activity at ∼200 °C.[16] Considering the potential applications of copper-based materials, many kinds of morphologies have been reported, such as wires, monodisperse nanocubes, octahedral nanocages, hollow nanospheres, and so forth.[15,17,18] Typically, the Zeng group used a solvothermal method in *N*,*N*-dimethylformamide (DMF) at 150−180 °C for 20−40 h to get hollow Cu_2O nanospheres. They found the formation process of Cu_2O hollow spheres included formation of CuO nanocrystals, aggregation of primary CuO nanocrystals, and the reductive transformation to Cu_2O.[15c] On the basis of the previous work on the preparation of Cu_2O nanostructures, we introduce a low temperature solution-phase method to synthesize nearly monodisperse Cu_2O nanospheres with controlled diameter and crystallization and then transform them to CuO nanospheres by gas-phase oxidation. Monodisperse Cu_2O or CuO nanospheres which can form three-dimensional self-assembly patterns should have potential usage on gas sensors because they have sufficient surface area and interspaces for gas absorption. Thus, their sensor properties have been explored in this communication.

Nearly Monodisperse Cu_2O Nanospheres. Typically, $Cu(CH_3COO)_2 \cdot H_2O$ (2 mmol, A.R., Tianjin BODI chemical reagent Co., Ltd.) was dissolved in 25 mL of DMF (A. R., Tianjin chemical reagent factory, containing ∼0.3% water), followed by the addition of poly(vinyl pyrrolidone) (PVP; 0.5−2 mmol, molecular weight = 30 000, C.R., Beijing chemical reagent Co., Ltd.) and $NaBH_4$ (0.01−0.3

* To whom all correspondence should be addressed. E-mail: ydli@tsinghua.edu.cn. Tel.: 86-10-62772350. Fax: 86-10-62788765.

(1) Joannopoulos, J. D.; Villeneuve, P. R.; Fan, S. *Nature* **1997**, *386*, 143.
(2) Caruso, F.; Caruso, R. A.; Mohwald, H. *Science* **1998**, *282*, 1111.
(3) (a) Matijevic, E. *Acc. Chem. Res.* **1981**, *14*, 22. (b) Matijevic, E. *Langmuir* **1994**, *10*, 8.
(4) Norris, D. J.; Vlasov, Y. A. *Adv. Mater.* **2001**, *13*, 371.
(5) Stöber, W.; Fink, A. *J. Colloid Interface Sci.* **1968**, *26*, 62.
(6) Xia, Y. N.; Gates, B.; Yin, Y. D.; Lu, Y. *Adv. Mater.* **2000**, *12*, 693.
(7) Zhang, H.; Cooper, A. I. *Chem. Mater.* **2002**, *14*, 4017.
(8) Egen, M.; Zentel, R. *Chem. Mater.* **2002**, *14*, 2176.
(9) Jiang, P.; Bertone, J. F.; Colvin, V. L. *Science* **2001**, *291*, 453.
(10) (a) Caruso, F. *Adv. Mater.* **2001**, *13*, 11. (b) Wang, D. Y.; Rogach, A. L.; Caruso, F. *Nano Lett.* **2002**, *2*, 857. (c) Wang, Y. J.; Caruso, F. *Chem. Mater.* **2005**, *17*, 953. (d) Schuetz, P.; Caruso, F. *Chem. Mater.* **2004**, *16*, 3066. (e) Cho, J.; Caruso, F. *Chem. Mater.* **2005**, *17*, 4547.
(11) (a) Jiang, X.; Herricks, T.; Xia, Y. N. *Adv. Mater.* **2003**, *15*, 1205. (b) Jeong, U.; Xia, Y. *Adv. Mater.* **2005**, *17*, 102. (c) Wang, Y.; Cai, L.; Xia, Y. *Adv. Mater.* **2005**, *17*, 473. (d) Wang, Y.; Xia, Y. *Nano. Lett.* **2004**, *4*, 2047.
(12) (a) Peng, Q.; Dong, Y. J.; Li, Y. D. *Angew. Chem., Int. Ed.* **2003**, *42*, 3027. (b) Peng, Q.; Xu, S.; Zhuang, Z. B.; Wang, X. Li, Y. D. *Small* **2004**, *1*, 216.
(13) (a) Sun, X. M.; Li, Y. D. *Angew. Chem., Int. Ed.* **2004**, *43*, 597. (b) Sun, X. M.; Li, Y. D. *Angew. Chem., Int. Ed.* **2004**, *43*, 3827. (c) Li, X. L.; Lou, T. J.; Sun, X. M.; Li, Y. D. *Inorg. Chem.* **2004**, *43*, 5442.
(14) (a) Deng, H.; Li, X. L.; Peng, Q.; Wang, X.; Chen, J.; Li, Y. D. *Angew. Chem., Int. Ed.* **2005**, *44*, 2782. (b) Wang, J. W.; Wang, X.; Peng, Q.; Li, Y. D. *Inorg. Chem.* **2004**, *43*, 7552.
(15) (a) Chang, Y.; Lye, M.; Zeng, H. *Langmuir* **2005**, *9*, 3746. (b) Liu, B.; Zeng, H. *J. Am. Chem. Soc.* **2004**, *126*, 8124. (c) Chang, Y.; Teo, J.; Zeng, H. *Langmuir* **2005**, *21*, 1074.
(16) Xu, J. Q.; Zhang, Q. F.; Fan, F. L. *Sensors Technology*; Harbin Institute of Technology Press: Harbin, China, 2004; p 92.
(17) (a) Wen, X.; Xie, Y.; Choi, C.; Wan, K.; Li, X.; Yang, S. *Langmuir* **2005**, *10*, 4729. (b) Zhao, Y.; Zhu, J.; Hong, J.; Bian, N.; Chen, H. *Eur. J. Inorg. Chem.* **2004**, 4072. (c) Gou, L.; Murphy, C. J. *Nano Lett.* **2003**, *3*, 231. (d) Wang, D.; Mo, M.; Yu, D.; Xu, L.; Li, F.; Qian, Y. T. *Cryst. Growth Des.* **2003**, *3*, 717. (e) Lu, C.; Qi, L.; Yang, J.; Wang, X.; Zhang, D.; Xie, J.; Ma, J. *Adv. Mater.* **2005**, *17*, 2562.
(18) (a) Muramatsu, A.; Sugimoto, T. *J. Colloid Interface Sci.* **1997**, *189*, 167. (b) Orel, Z. C.; Matijeviæ, E.; Goia, D. V. *J. Mater. Res.* **2003**, *18*, 1017.

10.1021/cm052256f CCC: $33.50
Published on Web 01/28/2006

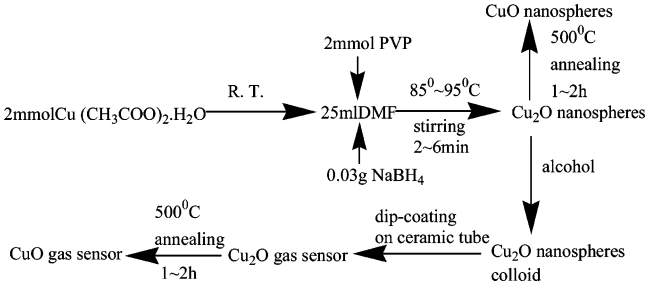

Figure 1. Flowchart of the nanospheres sample and sensor preparation details.

g, A. R., Tianjin chemical reagent factory). After stirring for several minutes, the mixture was heated to and maintained at 85−95 °C, and in 2−6 min, the color of the mixture was an orange color. The mixture was cooled to room temperature at once and washed by alcohol several times (Figure 1).

CuO Nanospheres. The spherical colloids of Cu_2O nanospheres were deposited on a Si wafer and dried in oven at 60 °C for 10 min. They were then transferred into the muffle furnace and heated at 500 °C for 1−2 h.

Scanning electron microscopy (SEM) images were taken using a field-emission microscope (Sirion FEI). Transmission electron microscopy (TEM) images were taken by a JEM-1200EX microscope operated at 120 kV. Electron diffraction (ED) patterns were taken by a Hitachi H800 (acceleration voltage 200 kV) and JEM-1200EX microscope operated at 120 kV. The X-ray diffraction (XRD) test was performed with a Bruker D8 Advance X-ray diffractometer with monochromatized Cu Kα radiation (λ = 1.5418 Å). The UV−vis spectra were obtained by a Hitachi U-3010 spectrophotometer. The gas sensitive properties were measured using a static test system made by Hanwei Electronics Co., Ltd., Henan Province, China.

In this communication, we introduce $NaBH_4$ as the reducing agent and DMF as the solvent. Differing from the reported formation mechanism on the preparation of Cu_2O hollow spheres by the Zeng group,[15c] $NaBH_4$, working as a strong reducing agent, reacts with a trace amount of H_2O in DMF and then reduces $Cu(CH_3COO)_2$ to Cu_2O nanocrystals. Under the low temperature of 80−90 °C, DMF, a weak reducing agent, acts merely as the solvent of this reaction. The chemical reaction is as follows:

$$4Cu^{2+} + BH_4^- + 5H_2O \xrightarrow[PVP]{DMF} 2Cu_2O(s) + B(OH)_3 + 2H_2 + 7H^+ \quad (1)$$

With the effect of DMF solvent and PVP, the primary Cu_2O nanocrystals prefer to aggregate into spherical nanospheres. The formation process of Cu_2O nanospheres can be identified by Figure 2A−C, which are obtained from the Cu_2O products collected at different aging times. Figure 2A shows the existence of small nanospheres during the process of aggregation to spherical morphology. With the increase of aging time, the nearly monodisperse nanospheres gradually come into being which can be confirmed by Figure 2B,C. The ED pattern of one Cu_2O nanosphere shown in Figure 2D confirms that the as-prepared Cu_2O nanospheres are the regular spherical aggregation of Cu_2O single-crystalline nanoparticles. The XRD pattern shown in Figure 1 of

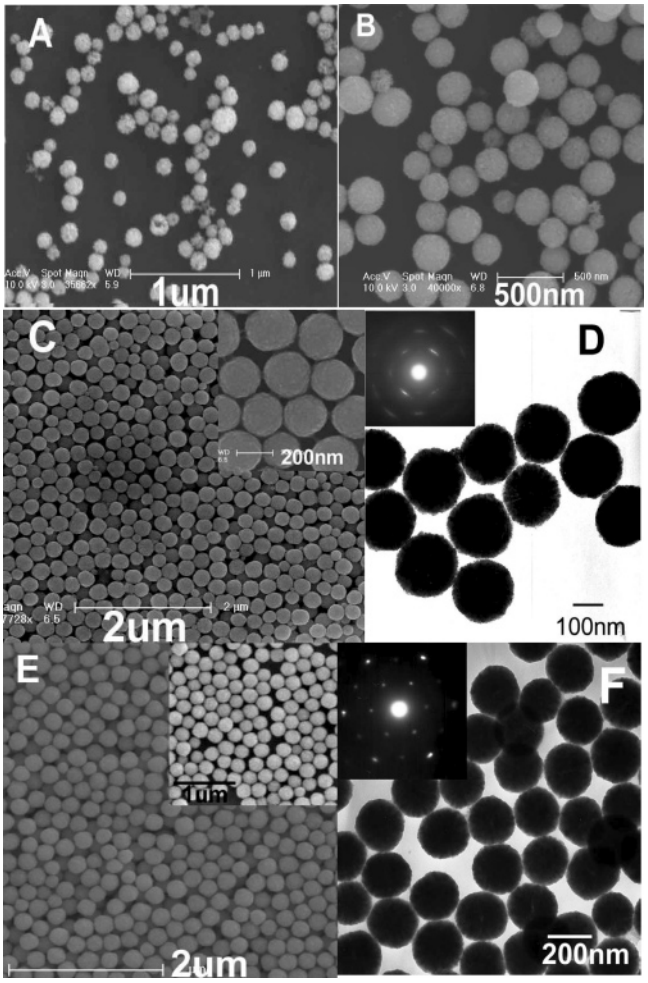

Figure 2. SEM images of Cu_2O nanospheres at different aging time: (A) 0.5, (B) 1.5, and (C) 3 min. The inset of part C shows the clear surface morphology of near-monodisperse Cu_2O nanospheres. Part D shows TEM and ED patterns of the nanospheres in part C. Parts E and F show the SEM, TEM, and ED patterns of nanospheres prepared by adding more appropriate H_2O.

Supporting Information identifies the pure cubic phase of Cu_2O (JCPDF 05-0667). The narrow size distribution of obtained nanospheres in Figure 2C can be demonstrated by Figure 2A of Supporting Information and mostly concentrates at the size of 200 nm. Most importantly, the properly high concentration of reactants is necessary for the supersaturation of uniform Cu_2O single-crystalline nanoparticles which can aggregate to be nearly monodisperse spherical colloids.[11d,15c] To confirm the reaction mechanism mentioned in eq 1, we add ∼0.05 mL of H_2O additionally to the same reaction system as above. As shown in Figure 2E,F, we gain single-crystalline Cu_2O nanospheres with improved monodispersity and the size distribution concentrates at ∼225 nm (Figure 2B, Supporting Information). This result is reasonable because, when adding an appropriate amount of additional water, the reaction velocity of eq 1 is increased and leads to the enhanced supersaturation of uniform Cu_2O nanoparticles. In the present case, Cu_2O nanoparticles could aggregate regularly to single-crystalline nanospheres with larger size. However, the addition of H_2O enables the larger nanospheres and makes the monodispersity worse. This can be identified by the SEM image shown in Figure 3 of Supporting Information. Thus, the proper quantity of H_2O is necessary

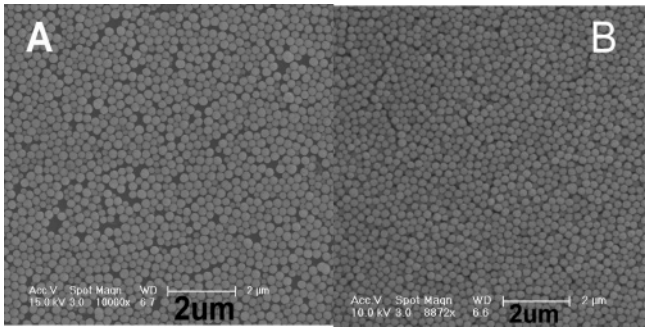

Figure 3. SEM images of two-dimensional (A) or three-dimensional (B) self-assembly modes of as-prepared Cu_2O nanospheres when spreading on Si wafer or ITO glass.

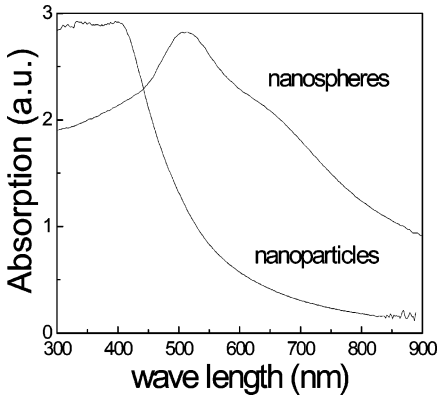

Figure 4. UV−vis absorption spectra of Cu_2O primary nanoparticles and near-monodisperse nanospheres.

for the kinetically controlled synthesis of monodisperse Cu_2O nanospheres. Of course, the optimal concentration of reagents, especially the concentration of H_2O in DMF, should be further studied. Because of the monodispersity of as-prepared Cu_2O nanospheres, as shown by the SEM images of Figure 3A,B, the two-dimensional or three-dimensional self-assembly pattern would spontaneously form when their alcohol colloids are spread on the Si or indium tin oxide (ITO) conductive glass substrate. This is perhaps attributed to the attractive capillary forces among the colloidal nanospheres. When the solvent evaporates slowly, these colloidal spheres are self-assembled into a closely packed array.[6,19]

As a p-type semiconductor, Cu_2O has been widely researched because it has the potential to form a solar cell with high open-circuit voltage by combination with a suitable n-type semiconductor. So the optical characterizations of the as-obtained Cu_2O nanosphere colloid have been carried out by the UV−vis absorption spectrum which was demonstrated in Figure 4. Differing from the nanoparticles which have an obvious absorption edge at ∼550 nm consistent with the reported band gap energy,[17] the prepared nanospheres of Cu_2O have a wide absorption peak at ∼520 nm. This result is consistent with many reported Cu_2O nanostructures.[20] It is mainly because when the Cu_2O nanoparticles aggregate to be nanospheres, the size becomes larger and uniform, and

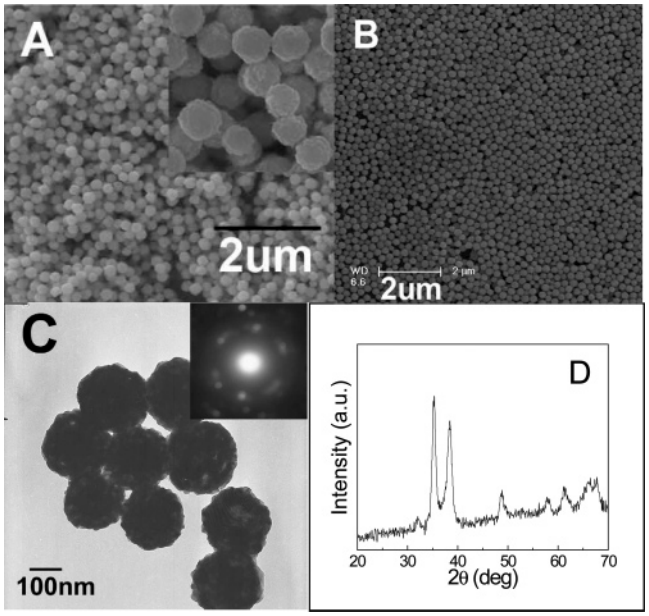

Figure 5. (A) SEM image of as-prepared CuO nanospheres with an inset of clear morphology of several nanospheres; (B) two-dimensional self-assembly pattern of CuO nanospheres; (C) TEM image of the CuO product with an inset to show the ED pattern of one nanosphere; and (D) XRD pattern of prepared CuO nanospheres.

then the scattering of visible light superimposes on the absorption of as-prepared nanospheres.

Considering the importance of the Cu-based materials family and the feasibility of chemical transformation between them, the CuO nanospheres were prepared by heat treatment of as-obtained Cu_2O nanospheres in a muffle furnace at 500 °C for 1−2 h. The SEM image in Figure 5A and TEM image in Figure 5C show that the nanospheres nearly have no shape evolution. Figure 5B shows the two-dimensional self-assembly state of CuO nanospheres. As shown in Figure 5C, the irregular diffraction dots in the ED pattern of one CuO nanosphere identify that CuO nanospheres are also the aggregation of single-crystalline nanoparticles. Clearly, the surface of the CuO nanospheres is more rough than that of Cu_2O nanospheres which may be helpful for their catalysis application. The XRD pattern in Figure 5D identifies that the product is monoclinic CuO (JCPDF 48-1548, Tenorite).

In recent years, many gas sensors based on copper oxides and n-type metal oxides have been researched, such as ZnO−CuO, SnO_2−CuO, and so forth. Typically, SnO_2 is sensitive to H_2S gas by the addition of a small amount of CuO because of the formation and the disruption of p−n junction.[21,22] Herein, we fabricated the gas sensors based on our prepared Cu_2O and CuO nanospheres only. Interestingly, we found they had high sensitivity to some gases, such as alcohol or gasoline.

The Cu_2O sensor was fabricated by dip-coating as-prepared Cu_2O alcohol colloids to the ceramic tube of the sensor body without an additional annealing process except for aging in the gas sensor system. Figure 6A shows the photograph of

(19) Denkov, N. D.; Velev, O. D.; Kralchevsky, P. A.; Ivanov, I. B.; Yoshimura, H.; Nagayama, K. *Nature* **1993**, *361*, 26.
(20) (a) He, P.; Shen, X.; Gao, H. *J. Colloid Interface Sci.* **2005**, *284*, 510. (b) Borgohain, K.; Murase, N.; Mahamuni, S. J. *Appl. Phys.* **2002**, *92*, 1292.
(21) (a) Kong, X. H.; Li, Y. D. *Sens. Actuators, B* **2005**, *105*, 449. (b) Choi, J. K.; Choi, G. M.; Man, G. *Sens. Actuators, B* **2000**, *69*, 120.
(22) (a) Chowdhuri, A.; Gupta, V.; Sreenivas, K.; Et al. *Appl. Phys. Lett.* **2004**, *84*, 1180. (b) Chowdhuri, A.; Gupta, V.; Sreenivas, K. *Sens. Actuators, B.* **2003**, *93*, 572. (c) Chowdhuri, A.; Sharma, P.; Gupta, V.; Et al. *J. Appl. Phys.* **2002**, *92*, 2172.

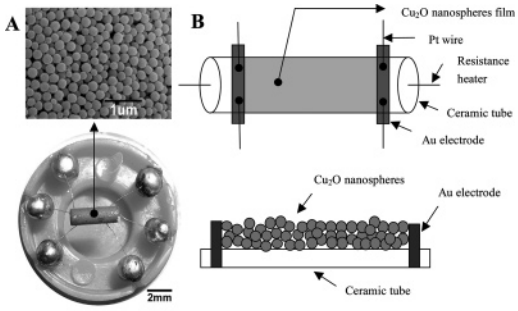

Figure 6. (A) Photograph of the gas sensor and the SEM image of thin films coated on it. (B) Schematic diagram showing the structure of a typical Cu_2O nanosphere gas sensor by top view and sectional view.

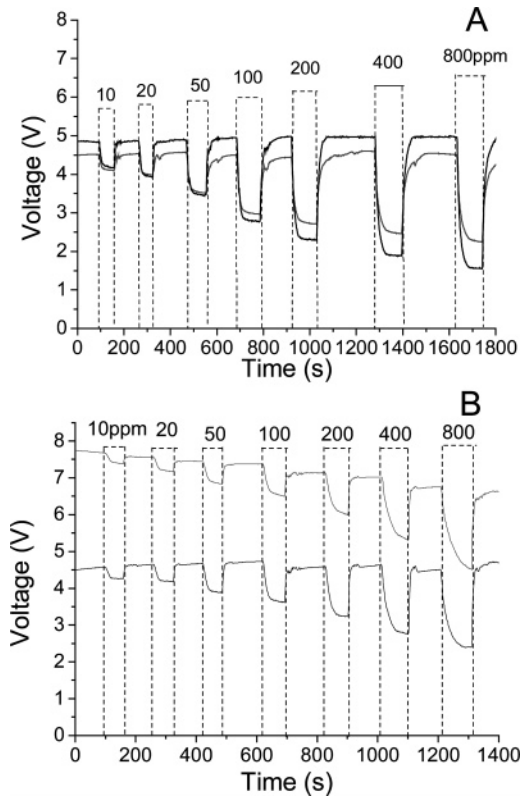

Figure 7. (A) Typical response curves of Cu_2O (black curve) and CuO (gray curve) nanosphere gas sensors to alcohol with increasing concentrations at 210 °C. (B) Typical response curves of Cu_2O octahedral microparticle (gray curve) and nanoparticle (black curve) gas sensors to alcohol with increasing concentrations at 210 °C.

a typical sensor and the SEM image of the Cu_2O nanospheres covering on it before the annealing process. Figure 6B shows the schematic diagram of the Cu_2O sensor structure and the sectional view. The CuO gas sensor was made by heat-treating the as-prepared Cu_2O sensor in a muffle stove at 500 °C for ~1 h. The nanosphere morphology was kept as a rough surface as shown in Figure 5A. From the SEM image shown in Figure 6A, it is clear that the nearly monodisperse nanospheres in the film can provide enough surface area and interspaces to contact the detected gas or atmosphere.

Figures 7A and 8A show the typical isothermal response curves of Cu_2O and CuO sensors when cycled by increasing alcohol and gasoline concentrations in ambient air with the range of 10−800 ppm, at a working temperature of 210 °C. For comparison with the prepared Cu_2O nanosphere gas sensors, we choose Cu_2O octahedral microparticle and

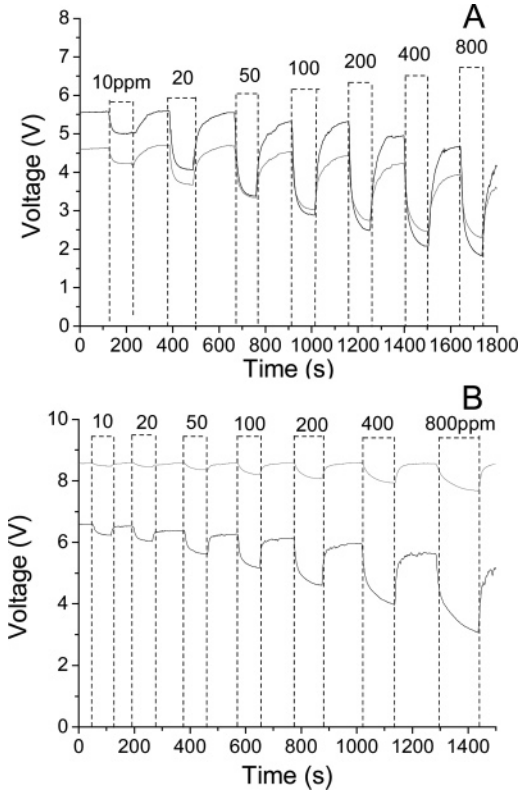

Figure 8. (A) Typical response curves of Cu_2O (black curve) and CuO (gray curve) nanosphere gas sensors to gas oil with increasing concentrations at 210 °C. (B) Typical response curves of Cu_2O octahedral microparticle (black curve) and nanoparticle (gray curve) gas sensors to gas oil with increasing concentrations at 210 °C.

nanoparticle alcohol colloids with the same concentration as the Cu_2O nanosphere colloid to make gas sensors by dip-coating and the same aging process. Their sensitivities to alcohol and gas oil have been demonstrated in Figures 7B and 8B. From these sensor results, it is evident that our as-prepared Cu_2O nanosphere sensor is much more sensitive than CuO, Cu_2O octahedral microparticle, and Cu_2O nanoparticle sensors. The Cu_2O nanosphere sensor offers a better response and quicker response/recovery time than many literature reports.[23] The resistance of the Cu_2O nanosphere sensor will decrease dramatically on the injection of ethanol or gasoline and reach its initial value quickly when releasing gases. The response time of the Cu_2O sensor is only ~15 s to alcohol and ~25 s to gasoline. The resume time of Cu_2O sensor also is only ~30 s for alcohol and ~45 s for gasoline. The detection limit of the as-prepared Cu_2O sensor can reach as little as several parts per million when detecting certain kinds of gas, such as alcohol or gasoline. On explaining these results, one important reason is that, in the Cu_2O nanosphere film coated on the sensor body, the monodispersity of single-crystalline Cu_2O nanospheres and their stacking mode result in larger surface area and much more capacious interspaces than any other shapes, which can provide sufficient space for the interaction between Cu_2O and detected gases. However, the Cu_2O microparticle film has less surface area and fewer active sites to contact with the gas. The SEM

(23) (a) Khatko, V.; Calderer, J.; Llobet, E.; Correig, X. *Sens. Actuators, B* **2005**, *109*, 128. (b) Gopal Reddy, C. V.; Cao, W.; Tan, O. K.; Et al. *Sens. Actuators, B* **2003**, *94*, 99.

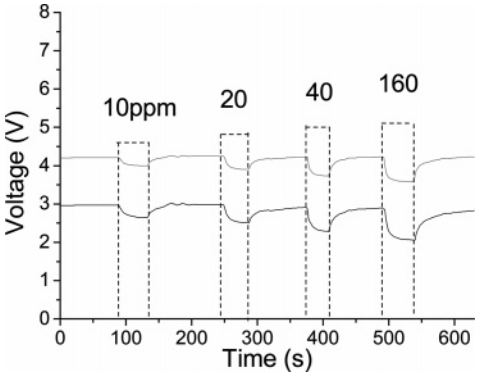

Figure 9. Typical response curves of Cu_2O (black curve) and CuO (gray curve) nanosphere gas sensors to H_2S with increasing concentrations at 210 °C.

image of the microparticle film is shown in Figure 4A of Supporting Information. For the Cu_2O nanoparticle film, as shown by the SEM image in Figure 4B of Supporting Information, although the nanoparticles have a smaller size than the nanospheres, their strong irregular aggregation also leads to fewer opportunities to contact the detected gas. Considering the selectivity of the as-prepared Cu_2O sensor, we have detected H_2S gas with the same concentration level at the working temperature of 210 °C, and the result is shown in Figure 9. From the response curve, we find it is not sensitive enough for practical usage and the voltage response is not proportional to the increasing concentration of H_2S.

The sensitivity difference of the Cu_2O and CuO nanosphere films perhaps is attributed to the reaction mechanism of Cu_2O or CuO to detected gases. When in contact with the reducing gas (electron donator), such as alcohol or gasoline, the negative charged oxygen (O^-, O^{2-}) absorbed on the Cu_2O or CuO nanosphere surface will react.[24] The reaction between the reducing gas and O^- or O^{2-} leads to the decrease of the carrier hole density in the surface charge layer and the increase of the Cu_2O or CuO resistance. Specifically, under the working temperature of 210 °C, the Cu_2O nanospheres absorb the oxygen in the air easier and then cover the surface with more active negatively charged oxygen (O^-, O^{2-}) than as-prepared CuO nanospheres. Different from the body formation, the surface Cu_2O formation was easily changed to be Cu_2O_{2-x} ($0 < x < 1$), an active transient state, which is more favorable for the interaction with reducing gases. When testing under lower temperature, they have bad sensitivity or even no sensitivity possibly as a result of the less active O^- and O^{2-} ions. This result is consistent with the theory by Gray et al. in 1948.[16] Of course, the radical mechanism about the high sensitivity of our as-prepared Cu_2O nansphere sensor should be further researched. Furthermore, as reported by much of the literature,[21−25] to enhance the selectivity of some gases and satisfy more applications, the work of noble metal doping on as-prepared nanospheres and preparation of core−shell structures, such as Cu_2O-SnO_2, Cu_2O-ZnO, $CuO-SnO_2$, and CuO−ZnO, should be further studied.

In summary, this communication shows an effective method to prepare nearly monodisperse Cu_2O and CuO nanospheres. The rapid production of supersaturated Cu_2O single-crystalline nanoparticles and their regular spherical aggregation lead to the monodispersity of Cu_2O nanospheres. By modulating the concentration of reactant H_2O, the diameter, crystallization, and monodispersity of Cu_2O nanospheres can be kinetically controlled. Because the thin films prepared by as-obtained nanospheres have big surface areas and plentiful spaces to interact with gases, the gas sensors based on as-prepared Cu_2O nanospheres have high sensitivity and good selectivity to some flammable gases. The surface modification with noble metals or n-type metal oxides based on obtained nanospheres will be more helpful to enrich their sensor applications.

Acknowledgment. This work was supported by NSFC (90406003), the Specialized Research Fund for the Doctoral Program of Higher Education, and the Foundation for the Author of National Excellent Doctoral Dissertation of P. R. China and the State Key Project of Fundamental Research for Nanomaterials and Nanostructures (2003CB716901).

Supporting Information Available: Typical XRD pattern of as-prepared nearly monodisperse Cu_2O nanospheres, different size distribution histograms of nearly monodisperse cuprous oxide nanospheres obtained by modulating the concentration of water, SEM image of as-obtained Cu_2O nanospheres when adding excess H_2O, and SEM images of octahedral microparticles and nanoparticles used for gas sensors (PDF). This material is available free of charge via the Internet at http://pubs.acs.org.

CM052256F

(24) Liu, J. F.; Wang, X.; Peng, Q.; Li, Y. D. *Adv. Mater.* **2005**, *17*, 764.

(25) Ivanov, P.; Llobet, E.; Vilanova, X.; Et al. *Sens. Actuators, B* **2004**, *99*, 201.